

Universal T/B scaling behavior of heavy fermion compounds

V. R. Shaginyan,^{1,2,*} A. Z. Msezane,² J. W. Clark,^{3,4} G. S. Japaridze,² and Y. S. Leevik⁵

¹*Petersburg Nuclear Physics Institute, NRC Kurchatov Institute, Gatchina, 188300, Russia*

²*Clark Atlanta University, Atlanta, GA 30314, USA*

³*McDonnell Center for the Space Sciences & Department of Physics,
Washington University, St. Louis, MO 63130, USA*

⁴*Centro de Investigação em Matemática e Aplicações,*

University of Madeira, 9020-105 Funchal, Madeira, Portugal

⁵*National Research University Higher School of Economics, St.Petersburg, 194100, Russia*

We address manifestations of T/B scaling behavior of heavy-fermion (HF) compounds, where T and B are respectively temperature and magnetic field. Using experimental data and the fermion condensation theory, we show that this scaling behavior is typical of HF compounds including HF metals, quasicrystals, and quantum spin liquids. We demonstrate that such scaling behavior holds down to the lowest temperature and field values, so that T/B varies in a wide range, provided the HF compound is located near the topological fermion condensation quantum phase transition (FCQPT). Due to the topological properties of FCQPT, the effective mass M^* exhibits a universal behavior, and diverges as T goes to zero. We also explain how to extract the universal scaling behavior from experimental data collected on different heavy-fermion compounds. As an example, we consider the HF metal YbCo_2Ge_4 , and show that its scaling behavior is violated at low temperatures. Our results obtained show good agreement with experimental facts.

PACS numbers: 71.27.+a, 71.10.Hf, 72.15.Eb

INTRODUCTION

Topological approach is a powerful method to gain information about a wide class of physical systems. Knowledge of the topological properties allows us to gain a general knowledge about physical systems without solving specific equations, which describe concrete systems and are often very complicated. As usually, the microscopic approach to a heavy fermion (HF) metal (for example, computer simulations) gives only particular information about specific solids, but not about universal features, inherent in the wide class of HF compounds. HF compounds can be viewed as the new state of matter, since their behavior near the topological fermion condensation quantum phase transition (FCQPT) acquire important similarities, making them universal. The idea of this phase transition, forming experimentally discovered flat bands, started long ago, in 1990 [1, 2]. At first, this idea seemed to be a curious mathematical exercise, and now it is proved to be rapidly expanding field with uncountable applications [1–9].

The scaling behavior of HF compounds is a challenging problem of condensed matter physics [6, 10–12]. It is generally assumed that scaling with respect to T/B (temperature-magnetic field ratio) is related to a quantum critical point (QCP) that represents the endpoint of a phase transition being tuned to $T = 0$ by such control parameters as magnetic field, pressure, and composition of the heavy-fermion compounds. As soon as the tuned endpoint of the phase transition reaches $T = 0$, it becomes a quantum phase transition (QPT). At the QCP, the associated quantum fluctuations involving valence, magnetism, charge, etc. can be expressed [11, 12]. Fluc-

tuations can also occur at second-order phase transitions, but the temperature range of these fluctuations is very narrow [13]; in contrast, T/B scaling can span a few orders of magnitude in T/B (as in Figs. 5 and 6) [6–8]. An attendant problem to be addressed by theory stems from the experimental finding that scaling behavior can take place without both QCP realization and effective-mass divergence [12]. To solve these problems, one needs to have a reliable theoretical framework for analysis of the observed phenomena.

A universal T/B scaling behavior is generated by quasiparticles belonging to flat bands, formed by topological FCQPT. In narrow electronic bands in which the Coulomb interaction energy becomes comparable to the bandwidth, interactions drive the topological FCQPT; as a result, at $T = 0$ flat bands are emerged, see e.g. [6–8]. Such flat bands in twisted graphene have been experimentally observed see e.g. [2]. Thus, we can safely use the model of homogeneous HF liquid, since we consider a behavior controlled by flat bands and related to the scaling of quantities such as the effective mass, heat capacity, magnetization, etc. As a result, the scaling properties are defined by momentum transfers that are small compared to momenta of the order of the reciprocal lattice length. The high momentum contributions can therefore be ignored by substituting the lattice for the jelly model; this observation is in a good agreement with experimental facts collected on many HF metals [6, 7, 9]. In our case quasiparticles are well defined excitations see e.g. [6, 7, 14], and the divergence of the effective mass M^* is not related to $Z \rightarrow 0$ (as it is can be assumed, see e.g. [15]), where Z is the quasiparticle amplitude. The divergence is defined by both the emergence of an

extended Van Hove singularities, pre-forming flat bands, and the Coulomb interaction, giving rise to strong correlations; as a result, at $T = 0$ the electronic dispersion becomes flat at the chemical potential μ , topologically transforming the Fermi surface into Fermi volume, see e.g. [1, 6, 7, 9, 16–18].

We show that the theory of fermion condensation (FC), which entails the topological FCQPT, provides the appropriate framework for describing and analyzing the universal scaling behavior of HF compounds [1, 3–7, 9]. We predict that T/B scaling behavior can be observed in a wide range of T/B values, provided the given HF compound is located near a topological FCQPT. Violation of T/B scaling at the lowest values of T/B is a signal that the given HF compound is situated prior to or before the FCQPT on the $T - B$ phase diagram, and hence exhibits Landau Fermi-Liquid (LFL) behavior at sufficiently low temperatures. The results of this theory are in good agreement with experimental observations collected on different strongly correlated Fermi systems like HF metals, quasicrystals and quantum magnets, holding quantum spin liquids [6, 7, 9].

SCALING BEHAVIOR OF THE EFFECTIVE MASS NEAR THE TOPOLOGICAL FCQPT

One of the main experimental manifestations of the topological FCQPT phenomenon is the scaling behavior of the physical properties of HF compounds located near such a phase transition. To understand this scaling behavior on a sound theoretical basis, we begin with a brief description of the associated behavior exhibited by the effective mass M^* in the framework of a homogeneous HF liquid [6]. This simplification avoids the complications associated with the anisotropy of solids and focuses of both the thermodynamic properties and the non-Fermi-liquid (NFL) behavior by calculating the effective mass $M^*(T, B)$ as a function of temperature T and magnetic field B [6–8], based on the Landau formula for the quasiparticle effective mass $M^*(T, H)$. The only modification introduced is that the effective mass is no longer approximately constant but now depends on temperature, magnetic field, and other parameters such as pressure, etc. We note that the FC theory is a good established theory based on the density functional theory; in that case, the Landau functional $E[n(\mathbf{p})]$ and the corresponding Eq. (1) are also derived in the same frameworks, therefore, being exact, see e.g. [4, 6, 7, 9, 16]. Here $n(\mathbf{p})$ is the quasiparticle distribution function.

At finite temperatures and magnetic fields, Landau's equation takes the form [6, 8, 19, 20]

$$\frac{1}{M_\sigma^*(T, H)} = \frac{1}{M} \quad (1)$$

$$+ \sum_{\sigma_1} \int \frac{\mathbf{p}_F \mathbf{p}}{p_F^3} F_{\sigma, \sigma_1}(\mathbf{p}_F, \mathbf{p}) \frac{\partial n_{\sigma_1}(\mathbf{p}, T, H)}{\partial p} \frac{d\mathbf{p}}{(2\pi)^3}$$

in terms of $n_\sigma(\mathbf{p})$ and the quasiparticle interaction F_{σ_1, σ_2} . The single-particle spectrum $\varepsilon(\mathbf{p}, T)$ is a variational derivative

$$\varepsilon_\sigma(\mathbf{p}) = \frac{\delta E[n(\mathbf{p})]}{\delta n_\sigma(\mathbf{p})}, \quad (2)$$

of the system energy $E[n_\sigma(\mathbf{p})]$ with respect to the quasiparticle distribution (or occupation numbers) $n_\sigma(\mathbf{p})$ for spin σ , which in turn is related the spectrum $\varepsilon_\sigma(\mathbf{p})$ by

$$n_\sigma(\mathbf{p}, T) = \left\{ 1 + \exp \left[\frac{(\varepsilon(\mathbf{p}, T) - \mu_\sigma)}{T} \right] \right\}^{-1}. \quad (3)$$

In our case, the chemical potential μ depends on spin due to the Zeeman splitting, $\mu_\sigma = \mu \pm \mu_B B$, where μ_B is the Bohr magneton. The magnetic field B appears in Eq. (3) via the ratio $\mu_\sigma/T = (\mu \pm \mu_B B)/T$. We note that (1) and (2) are exact equations [7, 16]. In our case, the Landau interaction F is fixed by the condition that the system is situated at a FCQPT. Its sole purpose is to bring the system to the topological FCQPT point, where $M^* \rightarrow \infty$ at $T = 0$ and $B = 0$, altering the topology of the Fermi surface, transforming it to a volume such that the effective mass acquires temperature and field dependence [6, 19, 21]. Provided the Landau interaction is an analytic function, at the Fermi surface the momentum-dependent part of the Landau interaction can be parameterized as a truncated power series $F = aq^2 + bq^3 + cq^4 + \dots$, where $\mathbf{q} = \mathbf{p}_1 - \mathbf{p}_2$, the variables \mathbf{p}_1 and \mathbf{p}_2 are momenta, and a, b , and c are fitting parameters defined by the condition that the system is at a FCQPT point.

Direct inspection of Eq. (1) shows that at $T = 0$ and $B = 0$, the sum of the first and second terms on the right side vanishes, since $1/M^*(T \rightarrow 0)$ goes to zero when the system is located at the FCQPT point. Given a Landau interaction analytic with respect to momenta variables, at finite T the right side of Eq. (1) is proportional $F'(M^*)^2 T^2$, where F' is the first derivative of $F(q)$ with respect to q at $q \rightarrow 0$. Results for the corresponding integrals can be found in textbooks – see especially Ref. [22]. At any rate, we have $1/M^* \propto (M^*)^2 T^2$ and arrive at [6, 7]

$$M^*(T) \simeq a_T T^{-2/3}. \quad (4)$$

At finite temperatures, application of a magnetic field $\mu_B B \gg k_B T$ drives the system to the LFL regime with

$$M^*(B) \simeq a_B B^{-2/3}, \quad (5)$$

where a_T and a_B are parameters and k_B the Boltzmann constant. If the system is still located before the FCQPT, the effective mass is finite $M^* = M_0$, and Eq. (5)

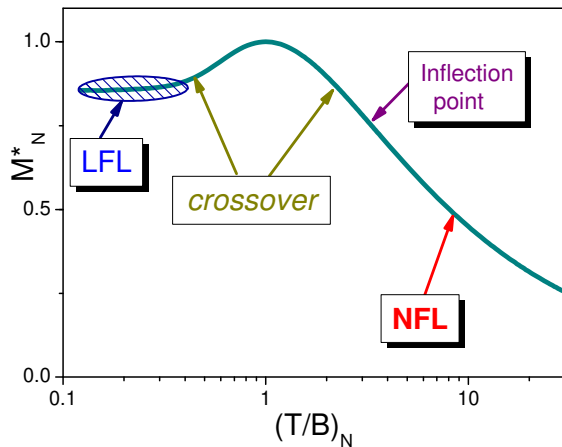


FIG. 1: (Color online). Scaling behavior of the dimensionless effective mass M_N^* versus dimensionless variable $(T/B)_N$. Scaling of thermodynamic properties is defined by M_N^* ; see Eq. (15). M_N^* is a function of $T_N \propto (T/B)_N \sim (T/B)/(T/B)_M$, as follows from Eq. (14). Solid curve depicts the scaling behavior M_N^* versus normalized temperature T_N as a function of magnetic field, given by Eqs. (8) and (12). Clearly, at finite $T_N < 1$ the normal Fermi liquid regime is realized. At $T_N \sim 1$ the system enters a crossover state, and at growing temperatures exhibits NFL behavior.

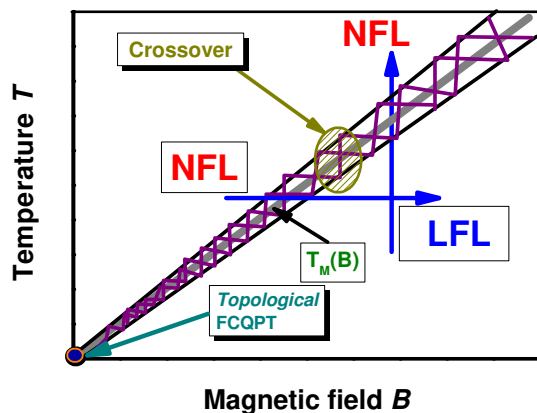


FIG. 2: (Color online). Schematic $T - B$ phase diagram of a HF compound, with magnetic field B as control parameter. The hatched area corresponds to the crossover domain at $T_M(B)$, given by Eq. (14). At fixed magnetic field and elevated temperature (vertical arrow) there is a LFL-NFL crossover. The horizontal arrow indicates a NFL-LFL transition at fixed temperature and elevated magnetic field. The topological FCQPT (shown in the panel) occurs at $T = 0$ and $B = 0$, where M^* diverges.

must be adjusted, since at $B \rightarrow 0$ the effective mass M^*

does not diverge; thus

$$M^*(B) \simeq a_B(B_0 + B)^{-2/3}. \quad (6)$$

From the Eq. (6) it follows that at some $B = B_0$ the effective mass becomes M_0 . Therefore, when $B \gg B_0$, the effective mass M^* depends on the magnetic field in accordance with Eq. (6), since the contribution coming from B defines the behavior of M^* . As a result, we can replace Eq. (5) by the equivalent equation

$$M^*(B) \simeq M_0 + a_B B^{-2/3}. \quad (7)$$

In the case of the HF liquid, these observations allow for construction of an approximate solution of Eq. (1) in the form $M^* = M^*(B, T)$ that satisfies both Eqs. (4) and (5). Introduction of “internal” scales simplifies the problem under consideration, allowing us to subdue the microscopic structure of the HF compounds under consideration [6, 7]. To establish such “internal” scales, we observe that near the FCQPT, the effective mass $M^*(B, T)$ reaches a maximum M_M^* at a certain temperature $T_M \propto B$. (See later comments on Eqs. (3) and (5) and Fig. 1). To conveniently measure the effective mass and temperature versus magnetic field B , we introduce the scales M_M^* and T_M , generating new variables $M_N^* = M^*/M_M^*$ (normalized effective mass) and $T_N = T/T_M$ (normalized temperature). In the vicinity of FCQPT, the normalized effective mass $M_N^*(T_N)$ is well approximated by a universal function [6, 7]

$$M_N^*(T_N) \approx c_0 \frac{1 + c_1 T_N^2}{1 + c_2 T_N^{8/3}}. \quad (8)$$

Here, $T_N = T/T_M \propto T/B$ (see Fig. 1) and $c_0 = (1+c_2)/(1+c_1)$, with c_1 and c_2 free parameters. We stress that values of M_M^* and T_M are defined by the microscopic structure of the HF compound under study, while the normalized values M_N^* and T_N demonstrate the universal scaling exhibited by HF compounds located near the topological FCQPT, since this scaling is determined by the nature of both the phase transition and the model of homogeneous HF liquid; we note that these observations are in good agreement with experimental facts collected on HF compounds, see e.g. [6–9]. From Eqs. (5) and (8) it follows that

$$M_M^* \propto B^{-2/3} \propto T_M^{-2/3}; T/B \simeq T/T_N. \quad (9)$$

The Landau interaction $F_{\sigma, \sigma_1}(q)$ appearing in Eq. (1) can produce the characteristic topological form of the spectrum $\varepsilon(p) - \mu \propto (p - p_b)^2 (p - p_F)$, with $(p_b < p_F)$ and $(p_F - p_b)/p_F \ll 1$, leading to $M^* \propto T^{-1/2}$ and creating a quantum critical point [23]. The same critical point is generated by the interaction $F(q)$ as represented by a non-analytic but integrable-over- x function with $x = q = \sqrt{p_1^2 + p_2^2 - 2xp_1p_2}$ and $F(q \rightarrow 0) \rightarrow \infty$ [4, 6, 8]. Both cases lead to $M^* \propto T^{-1/2}$, and Eq. (4) becomes

$$M^*(T) \simeq a_T T^{-1/2}. \quad (10)$$

In the same way, we obtain

$$M^*(B) \simeq a_B B^{-1/2}, \quad (11)$$

in terms of parameters a_T and a_B .

Taking into account the fact that Eq. (10) leads to a spiky density of states (DOS), with the spiky character fading away under increasing temperature as observed in quasicrystals [24–26], we note that the general form of $\varepsilon(p)$ produces the behavior of M^* given by Eqs. (10) and (11). This is realized in quasicrystals, which can be viewed as a generalized form of common crystals [24]. We note further that the behavior $1/M^* \propto \chi^{-1} \propto T^{1/2}$ is in good agreement with the behavior $\chi^{-1} \propto T^{0.51}$ observed experimentally [24, 26]. Our result $1/M^* \propto T^{1/2}$ is consistent with the robustness of the exponent 0.51 under hydrostatic pressure [26]. This robustness is guaranteed by the unique singular density of states associated with the topological FCQPT, which survives under application of pressure [24–28]. To develop the consequences of the the solution of Eq. (1) at finite B and T near the FCQPT, we construct an approximate solution by interpolating between the LFL behavior described by Eq. (11) and the NFL behavior described by Eq. (10), model the universal scaling behavior $M_N^*(T_N \propto T/B)$ [24]

$$M_N^*(T_N) \approx c_0 \frac{1 + c_1 T_N^2}{1 + c_2 T_N^{5/2}}, \quad (12)$$

with $c_0 = (1+c_2)/(1+c_1)$ and c_1, c_2 as fitting parameters. Taking into account Eqs. (11) and (12), we arrive at

$$M_M^* \propto B^{-1/2} \propto T_M^{-1/2}. \quad (13)$$

It follows from Eqs. (3), (8), and (12) that

$$T_M \propto B; T_N = \frac{T}{T_M} = \frac{T}{a_1 \mu_B B} \propto \frac{T}{B} \sim \left(\frac{T}{B}\right)_N. \quad (14)$$

Here a_1 is a dimensionless factor, μ_B is the Bohr magneton, $(T/B)_N = (T/B)/(T/B)_M$, where $(T/B)_M$ is the point at which M_N^* reaches its maximum value $M_N^* = 1$, as illustrated in Fig. 1. Expression (14) shows that Eqs. (8) and (12) determine the effective-mass scaling in terms of T and B . We conclude from Eq. (14) that since $T_M \propto B$, the curves $M_N^*(T, B)$ merge into a single curve $M_N^*(T_N = T/B)$, with $T_N = T/T_M = T/B$, demonstrating the widespread scaling in HF metals (for example, see [6, 7]). Such behavior is depicted in Fig. 1. We note that Eqs. (8) and (14) allow us to describe the behavior of the strongly correlated quantum spin liquid (SCQSL) existing in different frustrated magnets [6, 7].

Another important feature of the FC state is that apart from the fact that the Landau quasiparticle effectively acquires dependence on external factors such as the temperature and magnetic field, all the fundamental relations

inherent in the LFL approach remain formally intact. In particular, the famous LFL relation [6, 7, 20, 22],

$$M^*(B, T) \propto \chi(B, T) \propto \frac{C(B, T)}{T}, \quad (15)$$

still holds. Expression (15) is valid in the case of HF compounds located near a topological FCQPT, where the specific heat C , magnetic susceptibility χ , and effective mass M^* depend on T and B . Based on Eq. (15), we find that the normalized values of C/T and χ are of the form [6, 7]

$$M_N^*(B, T) = \chi_N(B, T) = \left(\frac{C(B, T)}{T}\right)_N. \quad (16)$$

It is seen from Eq. (16) that the aforementioned thermodynamic properties have the same scaling behavior as depicted in Fig. 1. Moreover, we shall see below that the thermodynamic properties of HF metals, SCQSL of frustrated magnets, and the other HF compounds exhibit the same scaling. Based on Eq. (8) and Fig. 1, we can construct the general schematic $T - B$ phase diagram of SCQSL, reported in Fig. 2. We assume here that at $T = 0$ and $B = 0$ the system is approximately located at a FCQPT point. At fixed temperature the system is driven by the magnetic field B along the horizontal arrow (from the NFL to the LFL parts of the phase diagram). At fixed B and elevated T the system moves from the LFL to the NFL regime along the vertical arrow. The hatched area indicating the crossover between LFL and NFL phases separates the NFL state from the paramagnetic slightly polarized LFL state. The crossover temperature $T_M(B)$ is given by Eq. (14).

T/B SCALING IN HEAVY FERMION COMPOUNDS

The experimentally based scaling behavior of M_N^* so derived is displayed in Fig. 1. Explanation of this scaling, $M_N^*(T_N) \propto C(B, T)/T$, presents a serious challenge to theories of the HF compounds. Most of the current theories analyze only the critical exponents that characterize $M_N^*(T_N)$ at $T_N \gg 1$ and thus consider only a part of the problem, missing the LFL and the transition regime [6, 7]. This scaling behavior of the effective mass M_N^* of HF compounds (or strongly correlated Fermi systems) is described by Eqs. (8) and (12). It follows then from Eqs. (15) and (16) that their thermodynamic properties must express the scaling behavior revealed by our analysis.

In the present context, the HF compounds are taken to represent strongly correlated Fermi systems as realized in HF metals, high- T_c superconductors, quasicrystals, SCQSL of frustrated magnets and two-dimensional liquids like ^3He . One can expect that HF compounds with their

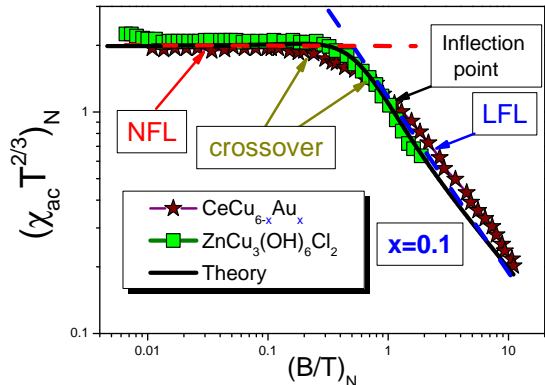


FIG. 3: (Color online). Universal B/T scaling of strongly correlated Fermi systems. Scaling of the HF metal $\text{CeCu}_{6-x}\text{Au}_x$ is extracted from data (measured at different field values $B = 0.05, 0.1, 0.3, 0.6, 0.9, 1.05$ T) in Ref. [30], and that of $\text{ZnCu}_3(\text{OH})_6\text{Cl}_2$ (measured at different field values $B = 0.5, 1.0, 3.0, 5.0, 7.0, 10.0, 14.0$ T), from data in Ref. [31]. At $B/T \ll 1$ the systems demonstrate NFL behavior with $\chi \propto M^*$ as given by Eq. (4), i.e., $T^{2/3}\chi \propto \text{const}$. At $B/T \gg 1$ the systems demonstrate LFL behavior with χ as given by Eq. (5), a decreasing function of B/T (see Eq. (12)). The NFL, crossover and LFL behavior are indicated by the arrows.

extremely diverse composition and microscopic structure would demonstrate very different thermodynamic, transport, and relaxation properties. To reveal the universal scaling behavior of HF compounds, irrespective of specific properties of individual compounds, we have introduced internal scales to measure the corresponding thermodynamic properties, as is done when we consider the scaling behavior of the effective mass M^* . This uniform behavior arises from the fact that HF compounds are located near a topological FCQPT, generating their uniform scaling behavior with respect to the effective mass M^* [6, 9, 29] (see Fig. 1). As an example, Fig. 3 displays the universal T/B scaling behavior of the HF metal $\text{CeCu}_{6-x}\text{Au}_x$ and the SCQSL of the frustrated insulator herbertsmithite $\text{ZnCu}_3(\text{OH})_6\text{Cl}_2$ [30, 31]. The existence of such universal behavior, exhibited by various and very distinctive strongly correlated Fermi systems, supports the conclusion that HF compounds represent a new state of matter [9, 29]. In contrast to the situation for an ordinary quantum phase transition, this scaling, induced by a FCQPT, occurs up to high temperatures $T < T_f \sim 100$ K, since the NFL behavior is defined by quasiparticles (with M_N^* given by Eqs. (8) and (12)), rather than by fluctuations or Kondo lattice effects [6, 7].

Some remarks are in order here. A strongly correlated Fermi system can be situated after the topological FC-

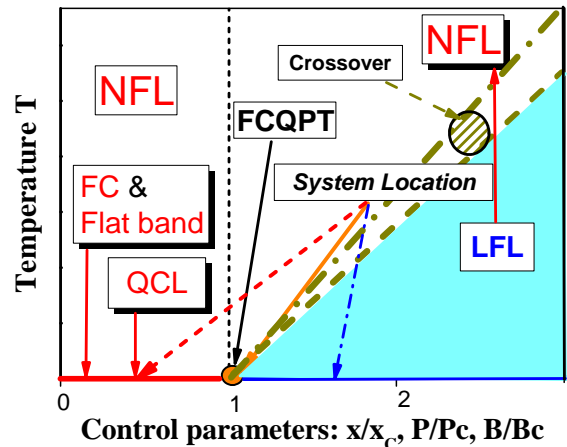


FIG. 4: (Color online). Schematic diagram of temperature versus these dimensionless control parameters: normalized pressure P/P_c , composition x/x_c , magnetic field B/B_c . We assume that $B_c > 0$, if $B_c = 0$, see the phase diagram 2. The solid black line indicates the topological FCQPT point (orange circle). At $T = 0$ and beyond the quantum critical line (QCL) implicating a flat band, as indicated by the red-dashed arrow. At any finite temperature $T < T_f$ and at elevated $P/P_c > 1$, $x/x_c > 1$, $B/B_c > 1$, the system enters the crossover and, then, the LFL region. The blue dash-dot arrow points to the system as situated before the topological FCQPT, where at $T \rightarrow 0$ it exhibits LFL behavior with effective mass $M^* = M_0$. At elevated magnetic fields, the behavior of the effective mass is given by Eq. (7), and the scaling behavior is restored at $B > B_0$.

QPT, i.e., on the ordered side defined by the quantum critical line (QCL), as shown in the schematic phase diagram 4. As it is shown in Fig. 4, FCQPT can be tuned by dimensionless control parameters: Normalized pressure P/P_c , composition x/x_c , magnetic field B/B_c . Here we assume that the critical magnetic field $B_c > 0$. In the case of $B_c = 0$, see Fig. 2, demonstrating that at $T = 0$ and $B = 0$ the system is located at the topological FCQPT. Note that there can be two critical magnetic fields B_{c1} and B_{c2} , as it is in case of the HF metal $\text{Sr}_3\text{Ru}_2\text{O}_7$ [32, 33].

As it is seen from Fig. 4, at $T = 0$ the crossover region is absent, and the FC state is separated from the LFL region by the first order phase transition [6], for the FC state is characterized by special quantum topological number, being a new type of Fermi liquid [3]. At $T > 0$ there is the crossover rather than a phase transition [6]. One may expect that the T/B scaling is caused by features not related to the presence of a QCP and the divergence of M^* (see e.g. [12]). On the other hand, if the system in question is located before a FCQPT, as indicated by the dash-dot arrow in Fig. 4, it exhibits

LFL behavior even in the absence of a magnetic field B at low $T \rightarrow 0$. At elevated magnetic fields reaching $B \gg B_0$, Eqs. (5) and (11) are valid and the scaling behavior returns to that given by Eqs. (8) and (12). Thus, to witness the presence of both the scaling behavior and divergence of the effective mass in measurements on HF compounds, one has to carry out measurements at sufficiently low temperatures and magnetic fields. For instance, the HF metal CeRu_2Si_2 exhibits NFL behavior at low temperatures (down to 170 mK) and small magnetic fields ($B \simeq 0.02$ mT) comparable with the magnetic field of the Earth [34]. Measurements carried out under application of magnetic fields have led to the incorrect statement that CeRu_2Si_2 demonstrates LFL behavior at low temperatures (see [34] and references therein). We note that if the critical magnetic field B_c is finite, then the scaling behavior occurs versus $T/(B - B_c)$ [29].

VIOLATION OF SCALING BEHAVIOR

Now we consider the statement that the scaling behavior can be observed without the presence of both a QCP and a divergent effective mass [12]. The T/B scaling behaviors experimentally observed in measurements of the magnetization dM/dT on the HF metals YbCo_2Ge_4 and $\beta - \text{YbAlB}_4$ [11, 12] are displayed in Figs. 5 and 6. As follows from Eqs. (12), (13), and (15), the function $B^{1/2}dM/dT$ can be represented as

$$\frac{dM}{dT} = \int \frac{\partial \chi(B_1, T)}{\partial T} B_1 dB_1 = \frac{1}{T_M} \int \frac{dM_N^*(y)}{dy} y dy, \quad (17)$$

where $y = T/B$. Taking into account Eq. (13), we obtain $T_M \propto B^{1/2}$ and Eq. (17) then reads

$$B^{1/2} \frac{dM}{dT} = \frac{1}{T_M} \int \frac{dM_N^*(y)}{dy} y dy, \quad (18)$$

Thus, $B^{1/2}dM/dT$ is a function of only the variable T/B .

As seen from Figs. 5 and 6, Eq. (18) and the corresponding calculations, represented by the solid curve, are in good agreement with the data [8, 11, 12]. To calculate the LFL behavior of dM/dT taking place at $(T/B)_N \ll 1$, i.e., $T \ll B$, we use the well-known relation $dM/dT = dS/dB$. Taking into account Eq. (11), we obtain $dS/dB = M^*(B)T/dB \propto B^{-3/2}T$, as shown in Figs. 5 and 6. At $(T/B)_N \gg 1$, i.e., $B \ll T$, the system exhibits NFL behavior. Using Eq. (10), we arrive at

$$\frac{dM}{dT} = \int \frac{\chi(T)}{dT} dB \propto \int \frac{M^*(T)}{dT} dB \propto T^{-3/2}B. \quad (19)$$

This theoretical result is in good agreement with experimental observations [11, 12]. Accordingly, we conclude that the fermion-condensation theory correctly describes the scaling behavior, showing good agreement with the data.

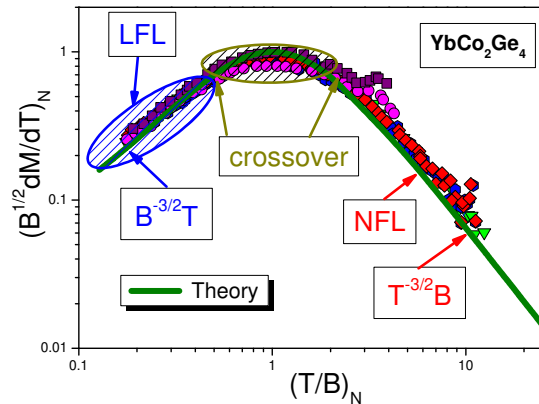


FIG. 5: (Color online). YbCo_2Ge_4 : Scaling behavior of the dimensionless normalized magnetization $(B^{1/2}dM(T, B)/dT)_N$ versus dimensionless $(T/B)_N$, measured at different field values $B = 0.05, 0.1, 0.2, 0.3, 0.5$ T. The data are extracted from measurements; see Fig. 4 of Ref. [12]. The NFL, crossover and LFL behavior are indicated by the arrows and hatched areas. The theory is represented by the solid curve, describing very well the scaling behavior of $(B^{1/2}dM(T, B)/dT)_N$ obtained in measurements on $\beta - \text{YbAlB}_4$ [11] (see Fig. 6). The LFL and NFL behaviors of $(B^{1/2}dM(T, B)/dT)_N$ are represented by $B^{-3/2}T$ and $T^{-3/2}B$, respectively.

Now we turn to the magnetic Grüneisen parameter $\Gamma_{mag}(T) = -(dM/dT)/C$ in the NFL regime, i.e., at $B \ll T$, with results reported in Fig. 7(a). It is seen that $\Gamma_{mag}(T)$ has an inflection point at $T = T_{inf}$, signaling that there is LFL behavior at lower temperatures rather than a divergence (see also Fig. 1). Thus, we assume that the HF metal YbCo_2Ge_4 is located before the topological FCQPT, as indicated by the dash-dot arrow in Fig. 4. We note that the inflection point takes place at too low temperatures and magnetic fields, and it could not make a visible impact on the scaling behavior reported in Fig. 5, that is, one needs to carry out measurements at sufficiently low T and B to clarify a possible violation of the scaling behavior. We suggest that YbCo_2Ge_4 can be tuned to FCQPT by the application of pressure or by doping, as it is done in the case of $\text{CeCu}_{6-x}\text{Au}_x$, while experimental facts show that $B_c = 0$ and the application of magnetic field drives YbCo_2Ge_4 from its QCP [12]. The LFL behavior of YbCo_2Ge_4 at $T \rightarrow 0$ is supported by the measurements of $\Gamma_{mag}(T)$, which exhibits divergent behavior $T^{-5/2}$ at the interval $T_{cr} \leq T \leq 0.8$ K, as it is seen from Fig. 7, where T_{cr} is the crossover temperature. At $T \leq T_{cr}$ the magnetic Grüneisen parameter $\Gamma_{mag}(T)$ does not follow the behavior indicated by the straight line because YbCo_2Ge_4 enters the crossover region (see Figs. 1 and 7). At the interval $T_{cr} \leq T \leq 0.8$ K

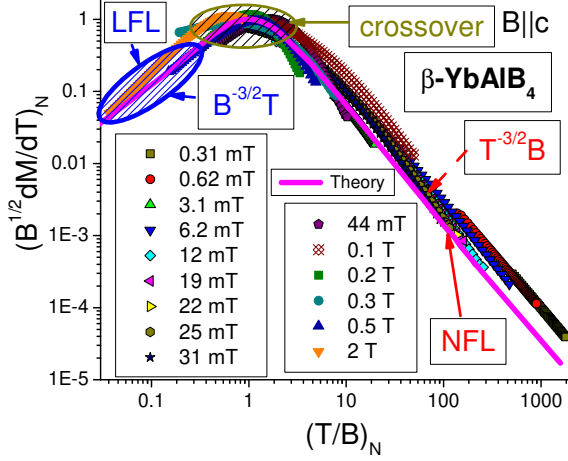


FIG. 6: (color online). Scaling behavior of the dimensionless normalized magnetization $(B^{1/2}dM/dT)_N$ versus the dimensionless normalized $(B/T)_N$ at different magnetic fields B shown in the legend [7, 8]. The data are extracted from measurements on $\beta - \text{YbAlB}_4$ [11]. The LFL behavior, crossover, and NFL behavior are indicated by the arrows. The theory is represented by the solid curve. Notation is specified in the caption of Fig. 5.

one has $\Gamma_{mag}(T) = -(dM/dT)/C \propto T^{-3/2}/T = T^{-5/2}$, since at $T \leq 0.8$ K and $B = 0$ the heat capacity C demonstrates LFL behavior, namely $C(T) \propto T$ [12]. It is seen from Fig. 7 that at $T \lesssim 0.15$ K, YbCo_2Ge_4 exhibits LFL behavior induced by the application of magnetic field $B = 0.1$. This behavior qualitatively resembles that occurring at $B = 0.05$ T.

Thus, we predict that at lower temperatures, $\Gamma_{mag}(T)$ will also exhibit LFL behavior. The measurements of dM/dT depicted in Fig. 8 support this conclusion: at $T \geq T_{cr}$, one finds $dM/dT \propto T^{-3/2}$ (see also Figs. 5 and 6), while at $T \leq T_{cr}$ the divergent behavior disappears. It is seen from Fig. 8 that dM/dT deviates from a straight line for $T \leq T_{cr}$, entering the crossover region and finally exhibiting LFL behavior (see Figs. 1 and 4). We note that the same behavior is seen in the frustrated magnet $\text{ZnCu}_3(\text{OH})_6\text{Cl}_2$, which hosts a quantum spin liquid and demonstrates LFL behavior at $T < 400$ mK [35]. The scaling behavior is expected to be violated in the LFL region, whereas it would be restored with growing temperatures $T > 400$ mK [36, 37]. It is seen from Fig. 3 that the scaling behavior is not violated at $(B/T) \geq 1$, for the measurements are taken at $T \geq 1.8$ K [31]. We expect the scaling violation at $T < 300$ mK and $B < 0.4$ T at the LFL behavior, see Fig. 3. As to YbCo_2Ge_4 , we suggest that measurements of the thermodynamic properties at very low temperatures and magnetic fields can clarify the physics of scaling behavior without the diver-

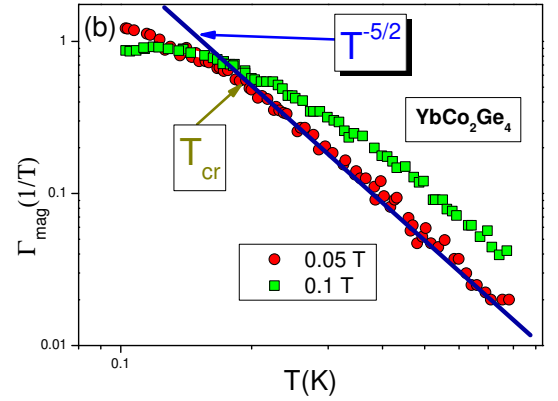
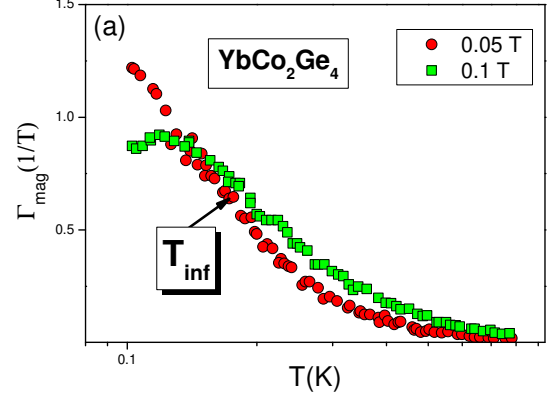


FIG. 7: (color online). Magnetic Grüneisen parameter $\Gamma_{mag}(T) = -(dM/dT)/C$ versus B for values shown in the legend. The data are taken from Ref. [12]. (a) $\Gamma_{mag}(T)$ versus a logarithmic temperature scale. The approximate location of the inflection point at temperature T_{inf} is indicated by the arrow. (b) $\Gamma_{mag}(T)$ is shown on a double-logarithmic plot. The solid line displays a $T^{-5/2}$ dependence at $B = 0.05$ T. At $T = T_{cr}$ YbCo_2Ge_4 enters the crossover, see Fig. 2, and the dependence $T^{-5/2}$ is vanished.

gence of the effective mass, for by now it is impossible to exclude the possibility of the scaling behavior down to the lowest temperatures.

CONCLUSION

The T/B scaling behavior of HF compounds has been investigated at some depth. It is shown that the HF metal YbCo_2Ge_4 does not exhibit scaling behavior down to lowest temperatures, since it is located before the topological fermion condensate quantum phase transition (FCQPT). For the same reason, the effective mass does

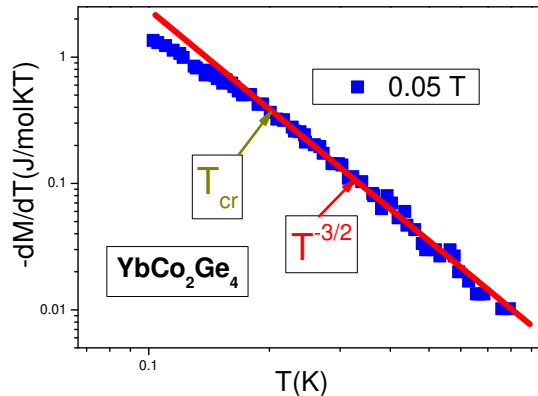


FIG. 8: (color online). The $-dM/dT$ NFL behavior at fixed field $B = 0.05$ T. The solid line indicates $T^{-3/2}$ dependence on a double-logarithmic plot. The experimental data are taken from Ref. [12]. The temperature T_{cr} at which the system enters the crossover region is indicated by the arrow. See also Fig. 1.

not diverge at the lowest temperatures. Based both on the theoretical consideration and the experimental facts, we have shown that there is no scaling without both the topological FCQPT and divergence of the effective mass. HF compounds exhibit the T/B scaling down to the lowest temperatures, provided these systems are located at the topological FCQPT. We suggest that measurements of the thermodynamic properties at very low temperatures and magnetic fields on YbCo_2Ge_4 can clarify the physics of scaling behavior without the divergence of the effective mass. We have also demonstrated that the topological fermion condensation theory gives a satisfactory description of the scaling behavior of various HF compounds. Our results are in good agreement with experimental observations.

ACKNOWLEDGEMENTS

We thank V. A. Khodel for stimulating and fruitful discussions. This work was partly supported by U.S. DOE, Division of Chemical Sciences, Office of Basic Energy Sciences, Office of Energy Research. JWC is indebted to the University of Madeira for gracious hospitality during periods of extended residence.

* Electronic address: vrshag@thd.pnpi.spb.ru

[1] V. A. Khodel and V. R. Shaginyan, JETP Lett. **51**, 553 (1990).

- [2] Y. Cao, V. Fatemi, S. Fang, K. Watanabe, T. Taniguchi, E. Kaxiras, and P. Jarillo-Herrero, Nature **556**, 43 (2018).
- [3] G. E. Volovik, JETP Lett. **bf 53**, 222 (1991).
- [4] V. A. Khodel and V. R. Shaginyan, V.V. Khodel, Phys. Rep. **bf 249**, 1 (1994).
- [5] G. E. Volovik, JETP Lett. **bf 107**, 516 (2018).
- [6] V.R. Shaginyan, M. Ya. Amusia, A. Z. Msezane, and K. G. Popov, Phys. Rep. **492**, 31 (2010).
- [7] M. Ya. Amusia, K. G. Popov, V. R. Shaginyan, and W. A. Stephanowich, *Theory of Heavy-Fermion Compounds*. Springer Series in Solid-State Sciences, Vol. **182** (Springer, Berlin, 2015)
- [8] V. R. Shaginyan, A. Z. Msezane, K. G. Popov, J. W. Clark, V. A. Khodel, and M. V. Zverev, Phys. Rev. B **93**, 205126 (2016).
- [9] M. Ya. Amusia and V. R. Shaginyan, *Strongly correlated Fermi systems: A new state of matter*. Springer Tracts in Modern Physics, Vol. **283** (Springer, Berlin, 2020).
- [10] Y. Matsumoto, S. Nakatsuji, K. Kuga, Y. Karaki, N. Horie, Y. Shimura, T. Sakakibara, A. H. Nevidomskyy, and P. Coleman, Science **331**, 316 (2011).
- [11] T. Tomita, K. Kuga, Y. Uwatoko, P. Coleman, S. Nakatsuji, Science **349**, 506 (2015).
- [12] A. Sakai, K. Kitagawa, K. Matsubayashi, M. Iwatani, and P. Gegenwart, Phys. Rev. B **94**, 041106(R) (2016).
- [13] E. M. Lifshitz and L. P. Pitaevskii, *Statistical Physics, Part 1*, (Butterworth-Heinemann, Oxford, 1996).
- [14] V. A. Khodel, J. W. Clark, M. V. Zverev, JETP Lett. **90**, 628 (2010).
- [15] C.M. Varma, Phys. Rev. Lett. **55**, 2723 (1985).
- [16] V. R. Shaginyan, Phys. Lett. A **249**, 237 (1998).
- [17] D. Yudin, D. Hirschmeier, H. Hafermann, O. Eriksson, A. I. Lichtenstein, and M. I. Katsnelson, Phys. Rev. Lett. **112**, 070403 (2014).
- [18] S. Link, S. Forti, A. Stöhr, K. Ksüter, M. Rösner, D. Hirschmeier, C. Chen, J. Avila, M. C. Asensio, A. A. Zakharov, T.O. Wehling, A. I. Lichtenstein, M. I. Katsnelson, and U. Starke, Phys. Rev. B **100**, 121407(R) (2019).
- [19] V. A. Khodel, J. W. Clark, M. V. Zverev, Physics of Atomic Nuclei **74**, 1237 (2011).
- [20] L. D. Landau, Zh. Eksp. Teor. Fiz. **30**, 1058 (1956).
- [21] J. W. Clark, V. A. Khodel, and M. V. Zverev, Phys. Rev. B **71**, 012401(2005).
- [22] E. M. Lifshitz, L. Pitaevskii, *Statistical Physics. Part 2*. (Butterworth-Heinemann, Oxford, 2002)
- [23] V. A. Khodel, M. V. Zverev, and J. W. Clark, JETP Lett. **81**, 315(2005).
- [24] V. R. Shaginyan, A. Z. Msezane, K. G. Popov, G. S. Japaridze, and V. A. Khodel, Phys. Rev. B **87**, 245122 (2013).
- [25] R. Widmer, P. Gröning, M. Feuerbacher, and O. Gröning, Phys. Rev. B **79**, 104202 (2009).
- [26] K. Deguchi, S. Matsukawa, N. K. Sato, T. Hattori, K. Ishida, H. Takakura, and T. Ishimasa, Nature Materials **11**, 1013 (2012).
- [27] T. Fujiwara and T. Yokokawa, Phys. Rev. Lett. **66**, 333 (1991).
- [28] T. Fujiwara, S. Yamamoto, and G. T. de Laissardière, Phys. Rev. Lett. **71**, 4166 (1993).
- [29] V. R. Shaginyan, V. A. Stephanovich, A. Z. Msezane, P. Schuck, J. W. Clark, M. Ya. Amusia, G. S. Japaridze, K. G. Popov, and E. V. Kirichenko, J. Low Temp. Phys.

- 189**, 410 (2017).
- [30] A. Schröder, G. Aeppli, R. Coldea, M. Adams, O. Stockert, H.v. Löhneysen, E. Bucher, R. Ramazashvili, and P. Coleman, *Nature* **407**, 351 (2000).
- [31] J. S. Helton, K. Matan, M. P. Shores, E. A. Nytko, B. M. Bartlett, Y. Qiu, D. G. Nocera, and Y. S. Lee, *Phys. Rev. Lett.* **104**, 147201 (2010).
- [32] V. R. Shaginyan, A. Z. Msezane, K. G. Popov, J. W. Clark, M. V. Zverev, and V.A. Khodel, *Phys. Lett. A* **377**, 2800 (2013).
- [33] V. R. Shaginyan, K. G. Popov, and V. A. Khodel, *Phys. Rev. B* **88**, 115103 (2013).
- [34] D. Takahashi, S. Abe, H. Mizuno, D. Tayurskii, K. Matsumoto, H. Suzuki, Y. Onuki, *Phys. Rev. B* **67**, 180407(R) (2003).
- [35] J. S. Helton, K. Matan, M. P. Shores, E. A. Nytko, B. M. Bartlett, Y. Yoshida, Y. Takano, A. Suslov, Y. Qiu, J.-H. Chung, D. G. Nocera, and Y. S. Lee, *Phys. Rev. Lett.* **98**, 107204 (2007).
- [36] V. R. Shaginyan, A. Z. Msezane, and K. G. Popov, *Phys. Rev. B* **84**, 060401(R) (2011).
- [37] V. R. Shaginyan, V. A. Stephanovich, A. Z. Msezane, G. S. Japaridze, J. W. Clark, M. Ya. Amusia, and E. V. Kirichenko, *J. Mater. Sci.* **55**, 2257 (2020).